SCIENTIFIC REPORTS
nature research

OPEN

# PAK1, PAK1Δ15, and PAK2: similarities, differences and mutual interactions

Dana Grebeňová, Aleš Holoubek, Pavla Röselová, Adam Obr, Barbora Brodská & Kateřina Kuželová*

**P21-activated kinases (PAK) are key effectors of the small GTPases Rac1 and Cdc42, as well as of Src family kinases. In particular, PAK1 has several well-documented roles, both kinase-dependent and kinase-independent, in cancer-related processes, such as cell proliferation, adhesion, and migration. However, PAK1 properties and functions have not been attributed to individual PAK1 isoforms: besides the full-length kinase (PAK1-full), a splicing variant lacking the exon 15 (PAK1Δ15) is annotated in protein databases. In addition, it is not clear if PAK1 and PAK2 are functionally overlapping. Using fluorescently tagged forms of human PAK1-full, PAK1Δ15, and PAK2, we analyzed their intracellular localization and mutual interactions. Effects of PAK inhibition (IPA-3, FRAX597) or depletion (siRNA) on cell-surface adhesion were monitored by real-time microimpedance measurement. Both PAK1Δ15 and PAK2, but not PAK1-full, were enriched in focal adhesions, indicating that the C-terminus might be important for PAK intracellular localization. Using coimmunoprecipitation, we documented direct interactions among the studied PAK group I members: PAK1 and PAK2 form homodimers, but all possible heterocomplexes were also detected. Interaction of PAK1Δ15 or PAK2 with PAK1-full was associated with extensive PAK1Δ15/PAK2 cleavage. The impedance measurements indicate, that PAK2 depletion slows down cell attachment to a surface, and that PAK1-full is involved in cell spreading. Altogether, our data suggest a complex interplay among different PAK group I members, which have non-redundant functions.**

PAK (p21-activated kinases) are a group of serine-threonine kinases originally identified as downstream effectors of p21 proteins, specifically of the Ras-related GTPases Rac1 and Cdc42[1,2]. The initial phase of PAK research focused on their role as small GTPase effectors in the context of dynamic remodelling of the cytoskeleton and of cell adhesion structures[3]. Later on, PAK were found to be involved in many cancer-related processes in different tumour types[4,5]. In parallel, the discovery of PAK1 nuclear localization[6] prompted the analysis of PAK functions in the cell nucleus.

The human PAK family is divided into the group I (PAK1 to PAK3) and group II (PAK4 to PAK6). In general, these kinases regulate the cytoskeleton dynamics, intracellular signaling, and gene expression[7]. The current knowledge about PAK group I is derived mostly from adherent cell models, where PAK activity usually correlates with increased cell motility. In this area, the research was mainly focused to PAK1, although some important differences between PAK1 and PAK2 have been reported[8]. In addition, PAK are known regulators of a wide range of cellular processes, including the dynamics of actin structures and microtubules, cell division, apoptosis, and adhesion to the extracellular matrix.

Despite considerable sequence homology within PAK group I, the individual members appear to have distinct function in cell physiology. Whereas PAK2 is more or less ubiquitiously expressed, PAK1 expression is more restricted in adulthood, and PAK3 is expressed mainly in the brain[9]. PAK2 and PAK4 are essential during embryonic development, since knockouts are embryonic lethal, at least in mice[9].

Group I PAK share some domains that are not present in the group II members[10,11]. In particular, the autoinhibitory domain (AID) is important for regulation of the kinase activity of the group I family members. The regulatory mechanism was described on the basis of PAK1 crystal structure[12], and is likely valid also for PAK2 and PAK3. PAK1 forms homodimers in a *trans* arrangement, the AID of one molecule interacting with the kinase domain of its partner molecule[13,14]. In this closed conformation, the kinase activity is very low. Binding of a

Department of Proteomics, Institute of Hematology and Blood Transfusion, U Nemocnice 1, 128 20, Prague, Czech Republic. *email: kuzelova@uhkt.cz

| Cat. No | Producer | Target | Immunogen | Type |
|---|---|---|---|---|
| #2602 | Cell Signaling | PAK1 | N-terminal peptide | rabbit polyclonal |
| ab40852 | Abcam | PAK1 | N-terminal peptide | rabbit monoclonal |
| ab223849 | Abcam | PAK1 | peptide within AA 200–300 | rabbit monoclonal |
| ab131522 | Abcam | PAK1 | region around AA 210–214 (P-V-T-P-T) | rabbit polyclonal |
| ab76293 | Abcam | PAK2 | N-terminal peptide AA 1–100 | rabbit monoclonal |
| ab40795 | Abcam | PAK group I pSer144/141 | sequence around the autophosphorylation site in PAK1 (pSer144) + PAK2 (pSer141) + PAK3 (pSer139) | rabbit monoclonal |
| ab75599 | Abcam | PAK1 pT212 | sequence around phosphorylated Thr212, not present in PAK2 | rabbit polyclonal |

**Table 1.** PAK antibodies used in the study.

small GTPase, like Rac1 or Cdc42, to the p21-binding domain (PBD) of PAK1 triggers conformation changes in the kinase domain, leading to dimer dissociation and to subsequent changes of conformation associated with increasing kinase activity[15]. Phosphorylation at Ser223 during this process was reported to be required for full PAK1 activation[16]. Autophosphorylation at PAK1 Ser144, or at the equivalent sites for the other PAK, stabilizes the open conformation and sustains high kinase activity. Mutation of tyrosines 131 or 429 is associated with reduced dimerization and enhanced kinase activity[17]. PAK3 homodimers, but also PAK1/PAK3 heterodimers were detected by co-immunoprecipitation of tagged proteins[18].

Apart from p21 proteins, PAK1 activity can be regulated by PxxP motif of SH3 domains[19] or through phosphorylation by Akt[20], JAK2[21,22], CDK1/cyclin B1[23], PDK1[24], or other kinases, which often regulate binding of phospholipids or scaffold molecules like GRB2 or NCK1.

Whereas PAK1 has been the predominant PAK group I member in studies focusing on the cell adhesion and migration, PAK2 was mainly studied in association with its role in the apoptosis. Upon PAK2 cleavage at a consensus caspase-3 site, the N-terminal fragment (28 kDa), containing the AID, dissociates from the C-terminal part (34 kDa), presumably inducing constitutive kinase activity[25]. Interestingly, *in vitro* studies suggest that the cleaved PAK2 molecules could remain in dimers[26]. Cells expressing a dominant-negative PAK2 were still able to undergo the apoptosis, but morphological changes, like membrane blebbing and formation of apoptotic bodies, were inhibited[25,27]. PAK2 cleavage induced by cellular stress occurs in a caspase-dependent manner[28–30], and contributes to apoptosis in various cell types. On the other hand, the full-length PAK2 has anti-apoptotic effects[31–33].

Human cancer is usually not associated with PAK mutation, but rather with a dysregulated PAK expression[7], especially with PAK1 and PAK4 overexpression. Both PAK1 and PAK4 genes are found on chromosomal regions that are frequently amplified in cancer[34]. PAK1 is the most studied and upregulated in cancers arising from PAK1-expressing tissues, such as brain, pancreas, colon, or ovary[7]. PAK activity has been linked to uncontrolled cell proliferation, altered cellular signaling, increased metastasis formation, and regulation of the immune system[35]. PAK overexpression was also associated with resistance to several drugs like paclitaxel, doxorubicin, cisplatin, and 5-fluorouracil[7,35]. Activating mutations of PAK1 also underlie neurodevelopmental disorders[17].

Given their role in tumour-related processes, PAK were proposed as possible targets in anti-cancer treatment[36–40]. However, with regard to specific functions of different family members, it will be necessary to search for more specific PAK inhibitors or to inhibit specific downstream effectors. This will require further studies of signaling pathways related to the individual PAK family members. Functional differences between PAK1 and PAK2 in relation to cell adhesion have been described in a human breast carcinoma cell line, using small interfering RNAs[8]. Although both PAK1 and PAK2 contributed to increased cell invasiveness, their roles were mediated by distinct signaling mechanisms. In addition, possible diversity is not limited to different family member genes: PAK1 has at least two confirmed splicing isoforms, denoted as PAK1A and PAK1B in the Swiss-Prot database, and little is known about their respective functions. Compared to the full length PAK1B (the transcript variant 1 according to the nomenclature of the National Center for Biotechnology Information, NCBI), the variant PAK1A (NCBI transcript variant 2) lacks the exon 15. In a melanoma model, overexpression of the shorter isoform (denoted as PAK1Δ15) did not trigger MAPK signaling and had no effect on the cell proliferation rate, in the opposition to the full-length form[41]. Furthermore, altered ratio between PAK1 and PAK1Δ15 in melanoma patients was associated with more aggressive disease and with worse prognosis.

In the present work, we compared the properties of the full-length PAK1, PAK1Δ15 and PAK2, focusing on their respective roles in the processes involved in the cell adhesion.

## Results

**Antibody characterization.** The expression level of PAK in HEK293T and HeLa cells was analyzed using a set of antibodies (Table 1). Whereas PAK2 was detected in a single dominant band at about 60 kDa, multiple bands were observed between 60 and 70 kDa using anti-PAK1 detection. Supplementary Fig. S1 shows a direct comparison of signals obtained using selected antibodies. At least three bands attributable to PAK1 were identified on large gels, with different relative intensities for different antibodies. PAK3 was not detected in any of the cell lines studied.

The specificity of the antibodies was further checked using siRNA-mediated PAK1/PAK2 silencing. As it is shown in Fig. 1a, all bands between 64 and 70 kDa were specific for PAK1, with the exception of those detected by

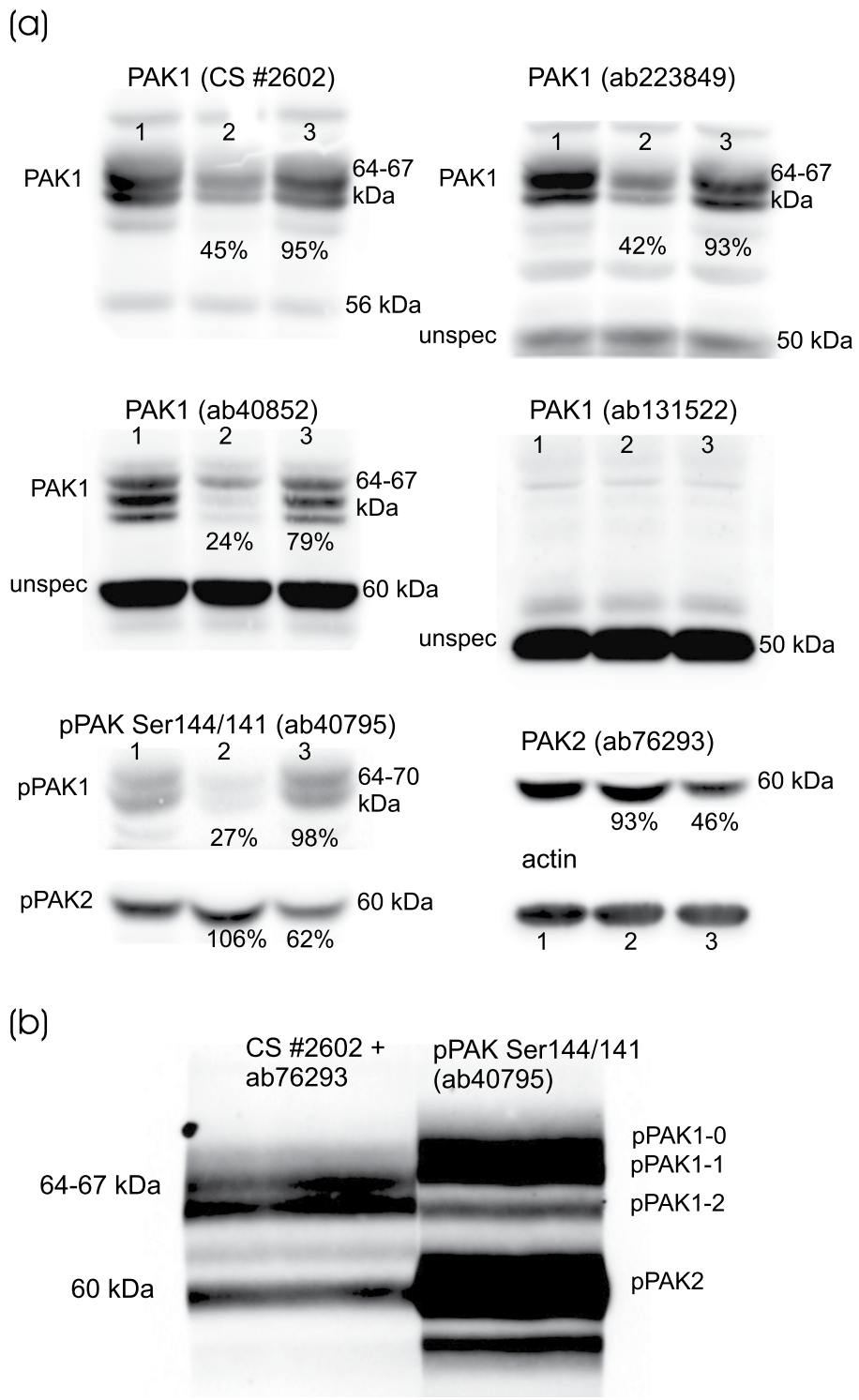


**Figure 1.** (**a**) Effect of siRNA PAK1/PAK2 on western-blot band intensity (antibody specificity control). HEK293T cells were transfected with siRNA targeting PAK1 or PAK2 and incubated for 48 h. The cell lysates were resolved on 18 × 18 cm gels and PAK expression was detected using different antibodies as indicated. Lanes: 1 – untransfected control, 2 – siRNA PAK1, 3 – siRNA PAK2. The band intensities for siRNA-treated samples were corrected using the loading controls (actin) and given as relative to the corresponding untransfected controls. (**b**) Direct comparison of signals from total PAK (PAK1 + PAK2, left) and pPAK Ser144/141 (right) antibodies. HEK293T cell lysate was resolved on a large gel, the proteins were transfered to a nitrocellulose membrane. The membrane was vertically cut, the individual parts were incubated with the indicated primary antibodies, then with the corresponding secondary antibody. The membrane was reassembled, covered with the chemiluminiscence substrate and the signal was recorded from both parts at once.

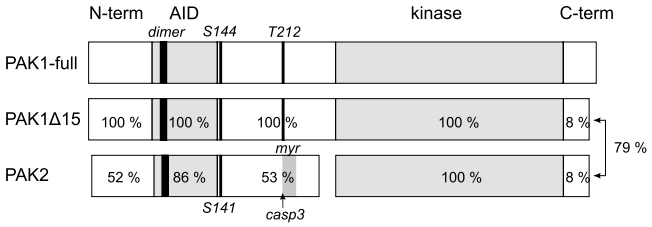


**Figure 2.** Schematic illustration of PAK group I structure. The numbers within the individual PAK1Δ15 and PAK2 domains indicate the sequence homology with the corresponding domains of the full-length PAK1. The dimerization sequence (dimer, AA 79–86) is identical for all three isoforms. The figure depicts the position of some important elements: the autoinhibitory domain (AID), the kinase domain (kinase), the autophosphorylation site S144/S141, the phosphorylation site T212, the cleavage site for caspase-3 (casp3) and the myristoylation region (myr). The C-terminal domains of PAK1Δ15 and PAK2 are similar to each other (79% homology), but different from that of PAK1-full. The scheme was created by the manuscript authors (KK).

ab131522, which gave no specific signal from the naturally occurring PAK. In addition, several strong unspecific signals were also identified for other antibodies, at lower molecular weight (MW). In general, the bands detected by phospho-specific antibodies were at slightly higher position compared to the total protein bands. The antibody recognizing the autophosphorylation site pSer144/141 on PAK1/PAK2, respectively, showed at least three PAK1 bands, which will be denoted as pPAK1-0, pPAK1-1 and pPAK1-2 in this study (Fig. 1b).

**PAK1 variants.** To further explore the nature of the observed PAK1 bands, we have constructed plasmids for exogenous expression of two PAK1 splicing variants[41]: the full-length isoform (PAK1-full) and the shorter variant lacking the exon 15 (PAK1Δ15). The sequence comparison of these two isoforms, along with PAK2 sequence, is given in the Supplementary Information (Supplementary Fig. S2). Some important sequence differences and the percentage of sequence homology for the individual domains are illustrated in Fig. 2. Due to a frameshift, the C-terminal part of PAK1Δ15 is different from that of PAK1-full. On the other hand, there is substantial similarity between the C-termini of PAK1Δ15 and PAK2. All PAK group I have an autoinhibitory domain (marked as "AID" in Fig. 2), which includes a dimerization sequence ("dimer"), and the kinase domain ("kinase"). The phosphorylatable threonine 212 (T212) is present in PAK1 variants, but not in PAK2. On the other hand, PAK2 is unique in having a cleavage site for caspases ("casp3"), followed by a myristoylation site ("myr")[42]. PAK1Δ15 amount in HEK293T cells was about ten times higher than that of PAK1-full when it was measured on the transcript level (Supplementary Fig. S3).

Figure 3 shows the position of new bands formed in cells transfected with plasmids coding for PAK1-full or PAK1Δ15. As all the used PAK1 antibodies target the N-terminal half of the protein, they should recognize both these variants equally. Indeed, the pattern of the exogenous bands was similar and the main difference was a shift towards lower MW due to the shorter C-terminal region of PAK1Δ15. The exogenous kinases appear little phosphorylated at Ser144, as no increase in the signal intensity after transfection was observed using the corresponding phospho-specific antibody (Fig. 3, ab40795). PAK1 Ser144 phosphorylation was even reduced to $70 \pm 16\%$ (mean and s.d. from 7 experiments) after transfection of plasmids for PAK1-full and to $61 \pm 10\%$ (mean and s.d. from 4 experiments) for PAK1Δ15. Interestingly, the exogenous proteins were also detected by the antibody ab131522, which did not recognize the endogenous PAK1 forms in HEK293T cells. On the other hand, only the higher bands from the exogenous products were apparent using the ab40852 antibody.

Both plasmids induced formation of at least two distinct bands. Previously, it was reported that PAK1 activation is associated with a change of its electrophoretic mobility, the activated form having higher apparent MW on polyacrylamide gels. The shift is generally supposed to be due to a hyperphosphorylation occurring during kinase activation. To verify this explanation, we analyzed the effect of alkaline phosphatase (AP) treatment of cell lysates on the band pattern (Fig. 4). The efficiency of AP treatment was confirmed by phospho-specific antibodies: signals from both pSer144/141 and pT212 were largely reduced in all AP-treated samples. However, the position of PAK1 bands was not substantially altered by the treatment. Instead, Fig. 4 suggests that the affinity of some of the PAK1 antibodies is affected by phosphorylation. Although a slight shift to the lower MW was usually detectable, the pattern of PAK1 bands was not substantially modified by AP treatment. The nature of different products formed from the transfected plasmids is thus not clear. Double bands were also obtained for fluorescently labeled PAK1 variants (see later).

**PAK dimerization.** PAK1 is assumed to form homodimers in a *trans* arrangement, where the kinase domain of one molecule is bound to AID of the other one. The kinase activity is low in this conformation and binding of a small GTPase to PAK1 regulatory domain is required for dimer dissociation and for full kinase activation. PAK2 homodimers are supposed to be formed as well, on the basis of sequence similarity and of indirect experimental confirmation[26]. PAK3 was reported to form both homodimers and PAK1/PAK3 heterodimers[18], but no data are available as to possible complexes involving PAK1 isoforms and PAK2. We thus constructed plasmids allowing for expression of eGFP- or mCherry-tagged PAK variants and analyzed their mutual interaction by co-immunoprecipitation. The exogenous proteins with their interaction partners were pulled down from HEK293T cell lysates using GFP/RFP Nano-Traps, and the presence of the co-precipitated forms was assessed through the complementary label (anti-RFP/GFP antibody, respectively). Representative western-blots

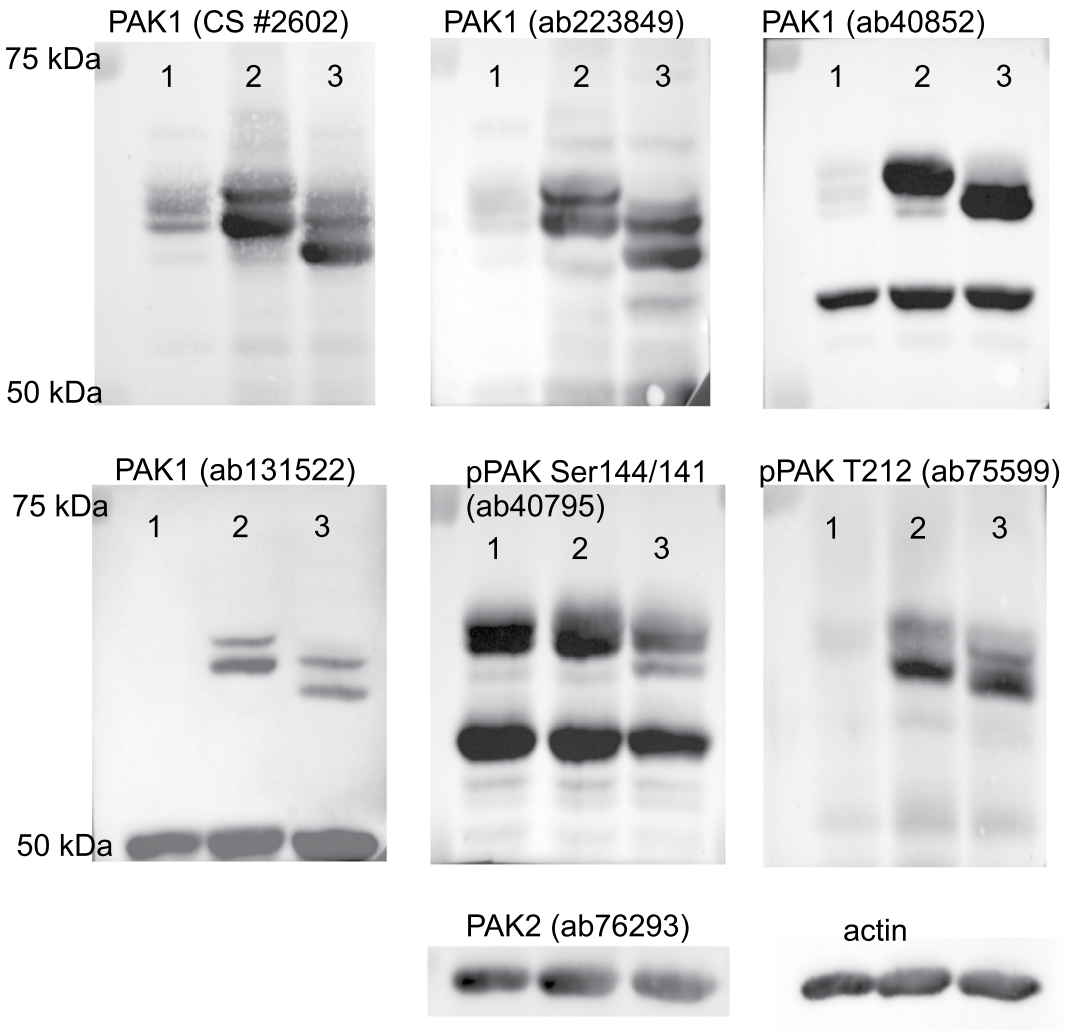


**Figure 3.** Band positions for the exogenous PAK1 forms. HEK293T cells were transfected with plasmids coding for PAK1-full or PAK1Δ15, incubated for 48 h and lysed. The proteins were resolved on 18 × 18 cm gels and blotted to nitrocellulose membranes, which were incubated with different antibodies as indicated. Lanes: 1 – untransfected cells, 2 – exogenous PAK1-full, 3 – exogenous PAK1Δ15.

from these experiments are shown in Fig. 5. The panel 5a documents the expected homodimer formation for PAK1-full, but also a strong interaction between PAK1-full and PAK2. Surprisingly, the formation of PAK1/PAK2 heterodimer was associated with PAK2 cleavage: although the GFP-labeled PAK1 is only slightly larger than the GFP-labeled PAK2, a marked difference between the position of the co-precipitated PAK1 and that of the co-precipitated PAK2 was found systematically (cf lane 2 versus lane 1 in the blot IP:RFP, WB:GFP). The truncated form of PAK2-GFP was also detectable in the cell lysates, exclusively in samples with PAK1 + PAK2 co-expression, but its amount was low (0.1 to 4%) compared to that of the intact PAK2-GFP (cf lane 2 with the other lanes in the input, WB: GFP). In the RFP-immunoprecipitates, the fragment represented the dominant PAK2-GFP form (93 to 95%): see the Supplementary Fig. S4 for direct comparison of the band position in the lysate and in the precipitate. Identical results were obtained using the inverse labeling, i.e. mCherry-labeled PAK2 and eGFP-labeled PAK1. Again, the interacting PAK2 was cleaved whereas PAK1-full was intact (Supplementary Fig. S5a). The length of the truncated PAK2 was reminiscent of the apoptotic fragment (p34), which is formed upon caspase-mediated PAK2 cleavage. As eGFP was added from the C-terminal side, the resulting fragment would have about 66 kDa. However, cell pretreatment with the caspase inhibitor Q-VD-OPh did not attenuate the cleavage (Supplementary Fig. S5b). Using the same approach, we found that PAK1-full interacts with PAK1Δ15, the latter kinase being cleaved in association with the complex formation (Fig. 5b). On the other hand, no cleavage was observed for PAK2 interaction with PAK1Δ15 (Fig. 5c). We have also directly proved that PAK2 forms homodimers (Fig. 5c, lane 1). The summary of the detected complexes is provided in Table 2.

The search for possible mixed endogenous/exogenous PAK complexes was complicated by the presence of shorter products formed from the plasmids. Nevertheless, a comparison of images obtained from anti-GFP and anti-PAK1 antibodies suggests that the endogenous PAK1 binds to PAK1-GFP (Supplementary Fig. S6). We have also noted that the phosphorylation of the endogenous PAK1 on Ser144 was reduced in the presence of

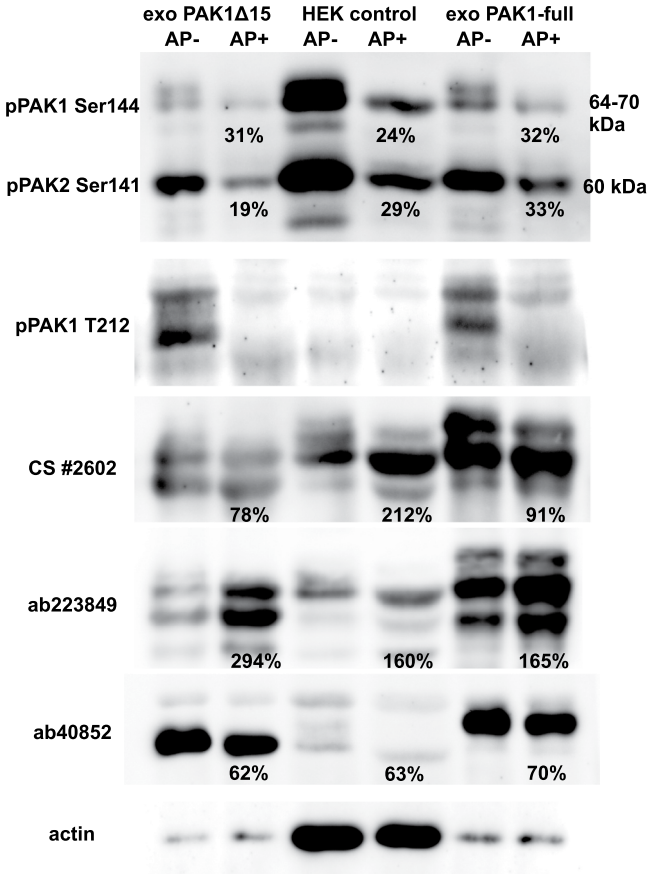


**Figure 4.** Effect of alkaline phosphatase treatment on western-blot bands of PAK. Lysates from HEK293T cells, control or transfected with plasmids coding for PAK1-full or PAK1Δ15, were incubated overnight with alkaline phosphatase (AP). The proteins were resolved on 18 × 18 cm gels and blotted to nitrocellulose membranes, which were incubated with different antibodies as indicated. The total protein load was five times lower in the lanes containing transfected cells than in those containing the control cells. The numbers indicate the band intensities in AP-treated samples as relative values compared to the corresponding untreated samples. In case of multiple bands, the signal from the sample was evaluated as a whole.

PAK1-full-GFP (panel b in Supplementary Fig. S6). This indicates that the exogenous PAK1-full interferes with the function of the endogenous protein, possibly through mixed dimer formation.

Complex formation was further analyzed using native electrophoresis. Lysates from cells transfected with PAK1-full-eGFP, PAK1Δ15-eGFP or PAK2-eGFP were prepared and resolved under non-denaturating conditions, transferred to a membrane and tested using anti-GFP antibody (Fig. 6). The position of PAK1Δ15 was only slightly higher compared to PAK2, in agreement with slightly larger MW. On the other hand, PAK1-full was not detectable in the native gels (Fig. 6, left part), probably because it was bound in multimolecular complexes, that are too large to enter the gel. The presence of PAK1-full in the cell lysates was confirmed under denaturing conditions (SDS electrophoresis), where the proteins migrate as monomers (Fig. 6, right part). Both PAK1-full and PAK1Δ15, but not PAK2, were always detected in double/multiple bands.

**Intracellular localization.** The fluorescently labeled forms of PAK1-full, PAK1Δ15 and PAK2 were further used to study the intracellular localization of the individual PAK group I members. The analysis was performed 24 to 48 h after HeLa cell transfection with the corresponding plasmids. For PAK1-full, we observed mainly a diffuse cytoplasmic staining, the signal being more intense in the proximity of the plasma membrane. Representative images of the localization of the exogenous PAKs at the cell-surface contact area are shown in Fig. 7 and in Supplementary Fig. S7. Both PAK1Δ15 and PAK2 were clearly enriched in focal adhesions, which were visualized either by paxillin/vinculin staining or using the interference reflection microscopy (IRM). In contrast, no accumulation of the fluorescence signal in adhesion points was noted for PAK1-full (Fig. 7a, bottom). When the cells were co-transfected with fluorescently labeled PAK1-full and PAK2/PAK1Δ15, the signal from PAK1-full was found beyond the adhesion points labeled with PAK2/PAK1Δ15 (Fig. 7b and Supplementary Fig. S7c). This corresponds to the known function of PAK1 in regulating dynamic actin structures inducing membrane protrusions.

Endogenous PAK were visualized by immunofluorescence. The only antibodies suitable for this application were ab76293, which is specific for PAK2, and the phospho-specific (pSer144/141) antibody detecting the autophosphorylated (kinase-active) forms of both PAK1 and PAK2. Since PAK1 expression level in HeLa cells was found to be very low (Supplementary Fig. S8), the signal of the phospho-specific antibody is mainly attributable

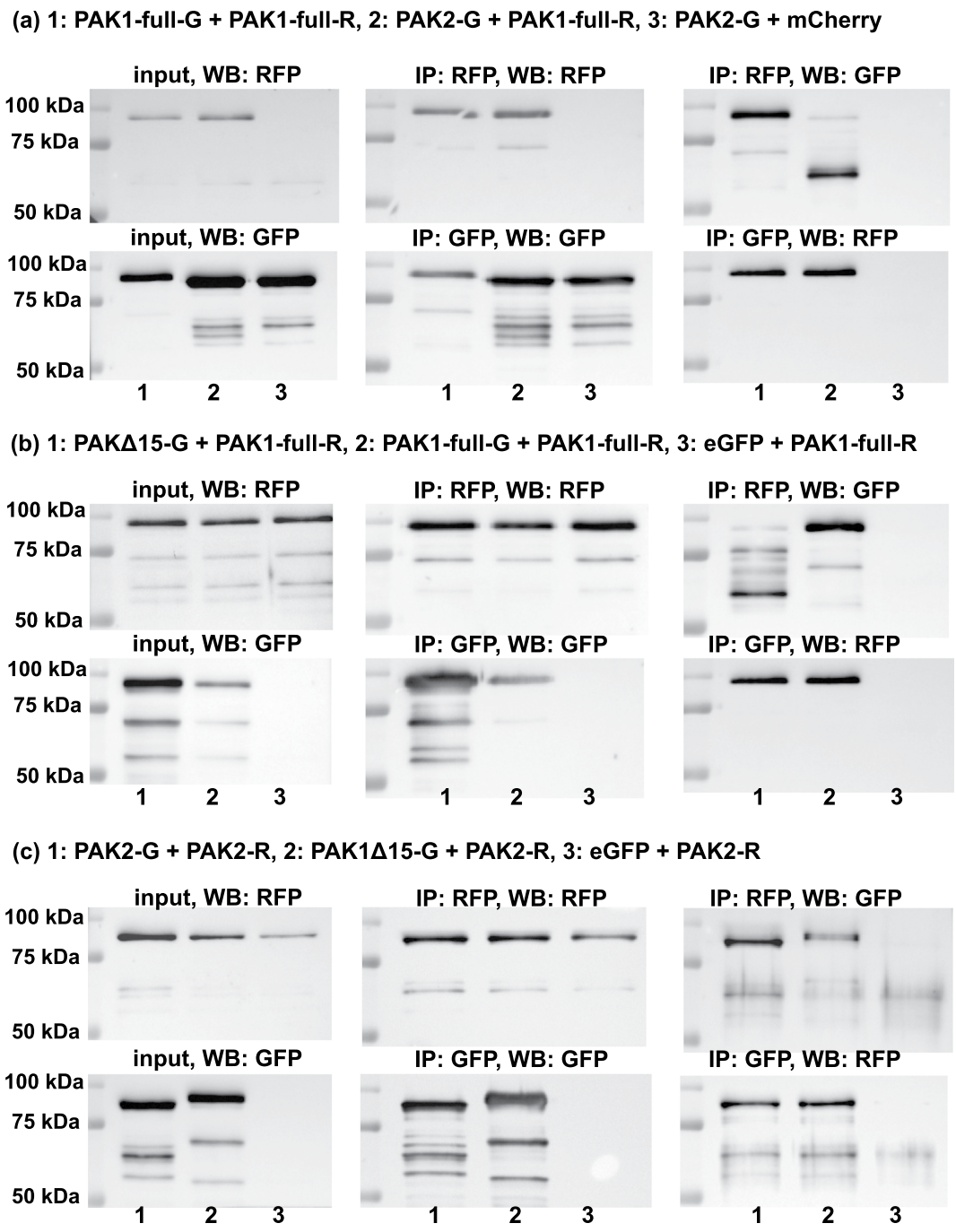


**Figure 5.** Results of co-immunoprecipitation experiments. HEK293T cells were cotransfected with combinations of labeled PAK isoforms (G-green variant, R-red variant) and empty eGFP/mCherry plasmids. Proteins were precipitated through GFP or RFP beads (indicated as IP:GFP or IP:RFP). The membranes were probed with anti-GFP or anti-RFP antibodies (indicated as WB:GFP or WB:RFP). The input (lysate) is also shown in the left column. MW markers are shown on the left of each blot. The uncropped images are included in Supplementary Fig. S16.

to PAK2 in HeLa cells. The specificity of PAK2 antibody signal from focal adhesions was confirmed by comparison with the GFP fluorescence from HeLa cells transfected with PAK2-GFP (Fig. 8a). Immunofluorescence staining of non-transfected cells confirmed the presence of the endogenous PAK2 in adhesion structures of HeLa cells (Fig. 8b). Moreover, we observed an intense staining of microtubule organizing centers (MTOC) in mitotic cells (Supplementary Fig. S9). In both HeLa and HEK293T cells, MTOCs were clearly labeled by pSer144/141 antibody, but not by PAK2 antibody. PAK1 binding to microtubules and to MTOC has already been observed previously and was related to T212 phosphorylation[23]. We did not detect any clear MTOC staining using the exogenous fluorescently labeled proteins. However, in HeLa cell line, mitotic cells were not present in the cell subpopulation expressing these proteins.

| | PAK1 full-length | PAK1Δ15 | PAK2 |
|---|---|---|---|
| PAK1 full-length | homodimers detected by co-IP | interaction detected by co-IP, PAK1Δ15 cleavage | interaction detected by co-IP, PAK2 cleavage |
| PAK1Δ15 | | homodimers indicated by native electrophoresis | interaction detected by co-IP, no cleavage |
| PAK2 | | | homodimers detected by co-IP |

**Table 2.** Summary of direct interactions among PAK group I proteins.

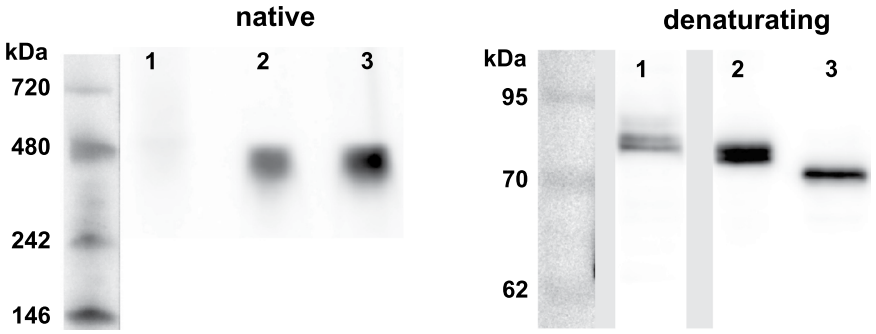


**Figure 6.** Analysis of PAK complex formation using native electrophoresis. HEK293T cell lysate from cells transfected with plasmids encoding PAK1-full-eGFP, PAK1Δ15-eGFP or PAK2-eGFP were resolved on electrophoretic gels under native (left) or denaturating conditions (right). MW markers (kDa) are shown on the left for both gels. For the denaturating conditions, one representative sample from several replicates, which were run in the same gel, is shown for each isoform. The full length gel is shown in Supplementary Fig. S16. Lanes: 1 – PAK1-full, 2 – PAK1Δ15, 3 – PAK2.

**Effect of small molecule inhibitors.** To analyze the impact of an acute inhibition of PAK, we employed the compound IPA-3, which binds covalently to the regulatory domain of PAK group I proteins. The efficiency of IPA-3 depends on the cell density[43] and we thus adhered to identical conditions in all experiments. Moreover, as IPA-3 causes oxidative stress, it is recommended to use a control compound, PIR3.5, which also induces oxidative stress, but does not alter PAK activity. We have verified that the toxicity of both inhibitors was similar over the used concentration range (Supplementary Fig. S10). For comparison, we used an alternative PAK inhibitor, FRAX597, which binds non-covalently to the ATP-binding site of PAK group I and prevents kinase activity[44]. No toxicity of 24 h FRAX597 treatment was observed up to 20 μM concentration. FRAX597 is less specific compared to IPA-3 as it inhibits other kinases in addition to PAK. IPA-3 is an allosteric inhibitor, which binds specifically to the inactive PAK forms and presumably inhibits also non-kinase functions of these proteins.

PAK1 is a known downstream effector of kinases of the Src family (SFK). We thus also evaluated the effects of dasatinib, a potent SFK inhibitor. We have shown previously that 100 nM dasatinib treatment completely blocked SFK activity in a few minutes[45] and we thus used this dose in all experiments presented in this study.

The efficiency of all inhibitors in blocking PAK kinase activity was assessed through the analysis of the extent of phosphorylation at the autophosphorylation site, which is present in both PAK1 (Ser144) and PAK2 (Ser141). Figure 9(a,b) shows changes in phosphorylation of Ser144/141 in cells treated for 30 min with IPA-3 or FRAX597. Examples of the detected chemiluminiscence signals for cells treated in suspension are given in Fig. 9a. In HEK293T cells, the effect of IPA-3 was evaluated separately for each PAK1 band defined in Fig. 1b. We noted considerable difference in IPA-3-induced effect between cells treated in suspension and cells treated in adhered monolayer (Fig. 9b). IPA-3 reduced Ser144/141 phosphorylation in cells treated in suspension (left), but not in monolayers (right). In suspension, the sensitivity of the individual PAK1 bands to IPA-3 decreased with increasing apparent MW. The control inhibitor, PIR3.5, did not induce PAK dephosphorylation at Ser144/141 (Supplementary Fig. S11). In HeLa cells, PAK1 was barely detectable and it was difficult to quantify any change in PAK1 phosphorylation. Nevertheless, the trend was similar as in HEK293T cells (Supplementary Fig. S11). Quite surprisingly, the effect of SFK inhibition by dasatinib on Ser144/141 phosphorylation was only moderate and it was comparable for all PAK isoforms and conditions (Fig. 9c). As expected, FRAX597 was the most efficient inhibitor of PAK kinase activity, inducing PAK1 Ser144 dephosphorylation by 70% at 4 μM concentration (Fig. 9a).

We have also noted that the decrease in Ser144 phosphorylation due to IPA-3 treatment was associated with an increase in PAK1 phosphorylation at both T212 and Ser20 in HEK293T cells (Supplementary Fig. S12).

**Monitoring of cell-surface interactions.** PAK group I are known to be involved in regulation of cell adhesion and migration. PAK1, as a downstream effector of SFK, promotes formation of membrane protrusions and releases the cytoskeletal tension, which is associated with a high stability of cell-surface adhesion points. The role of PAK2 in adhesion processes is much less explored, although differences between PAK1 and PAK2 have already been reported. Electrical Cell-Substrate Impedance Sensing (ECIS) is a powerful technique for real-time monitoring of cell interaction with a planar surface and we thus used this non-invasive method to study the cell

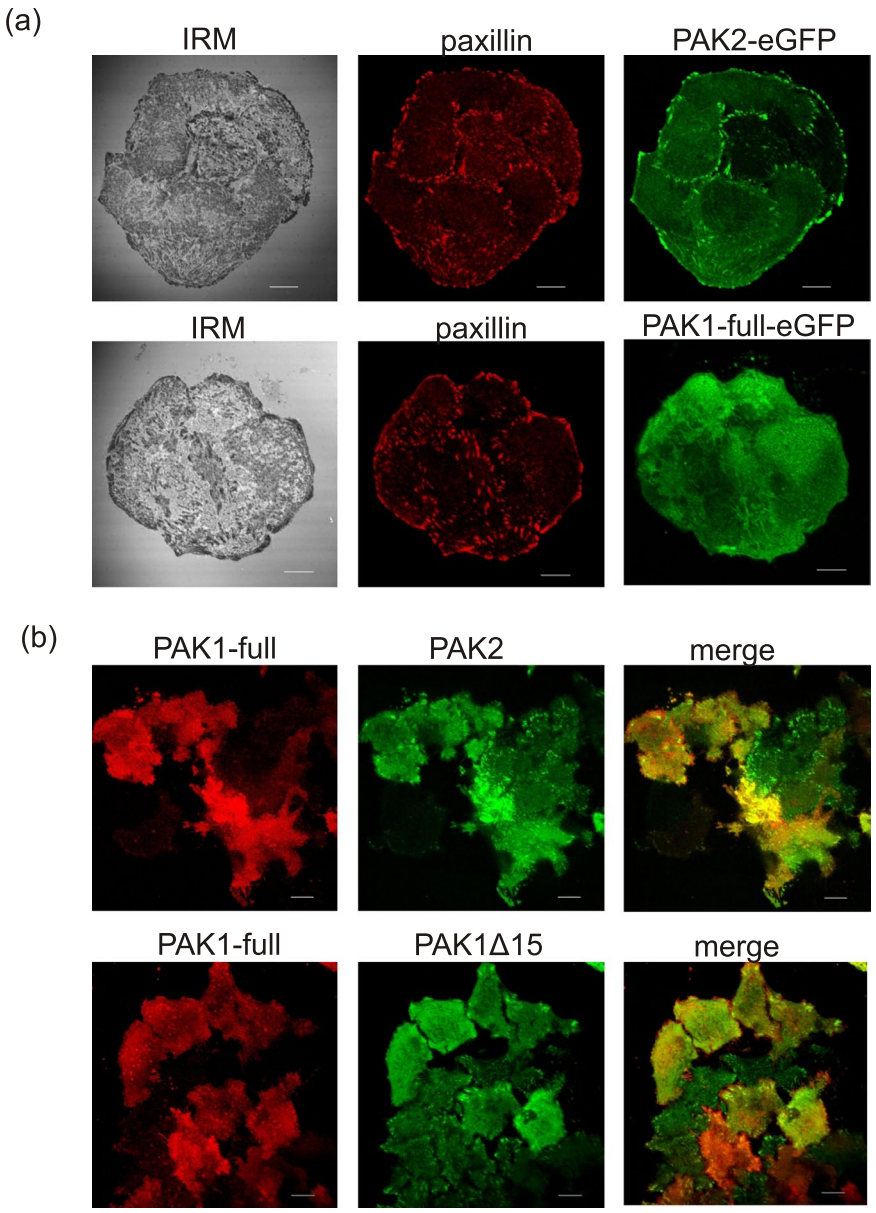


**Figure 7.** Analysis of PAK intracellular localization. HeLa cells were transfected with plasmids encoding fluorescently labeled variants of PAK1-full, PAK1Δ15, or PAK2, and the intracellular localization of the exogenous proteins at the cell-surface contact area was analyzed using confocal microscopy. (**a**) Top: Localization of PAK2-eGFP in cell-surface adhesion points, which were visualized by the interference reflection microscopy (IRM) or by paxillin immunofluorescence staining in fixed and permeabilized cells. Bottom: In contrast, no accumulation of PAK1-full-eGFP in paxillin-riched structures was found. (**b**) Analysis of the intracellular localization of PAK1Δ15/PAK2 (green) and PAK1 full-length (red) in co-transfected living cells. The scale bars correspond to 10 µm. Additional examples are given in the Supplementary Fig. S7.

response to inhibition of PAK or SFK activity. In the ECIS assay, gold microelectrodes embedded in the bottom of the testing plate enable to monitor cell binding to the well bottom through changes of the electrical impedance, which is further decomposed into resistance and capacitance.

Typical examples of ECIS records are given in Fig. 10. The measurement was performed in two different settings: the cells were either pretreated in suspension with the inhibitors for 30 min before seeding into the ECIS plate (setting 1) or treated after the cell attachment, during signal recording (setting 2). In the latter case, the time of inhibitor addition is marked with an arrow.

The largest changes occurred after dasatinib treatment (lines in magenta) and were indicative of decreased cell spreading. Indeed, microscopic analysis showed significant reduction of the cell area following dasatinib treatment in both cell lines (Supplementary Fig. S13). On the other hand, the effects of PIR3.5 were only mild: we usually observed faster signal growth in HEK293 cells pretreated with PIR3.5 (setting 1) compared to the

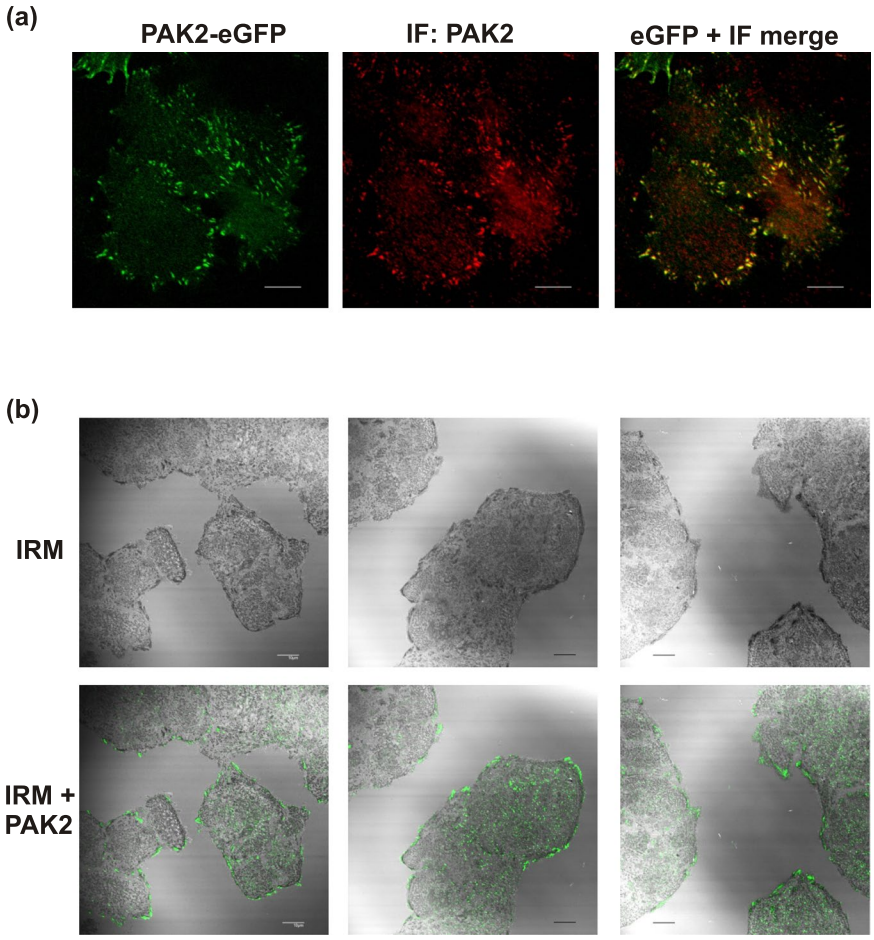


**Figure 8.** Analysis of endogenous PAK localization by immunofluorescence staining. (**a**) PAK2 antibody specificity control. The signal from PAK2 antibody, combined with an AlexaFluor647-conjugated secondary antibody, was compared with the eGFP signal in HeLa cells transfected with PAK2-eGFP. (**b**) Top: HeLa cell-surface adhesion points visualized by interference reflection microscopy (IRM) in untransfected cells. Bottom: PAK2 signal (green) is superposed on IRM signal from the same visual field. The scale bars correspond to 10 µm.

controls treated with solvent only. No reproducible change was detected in the setting 2, and no marked change was detected in HeLa cells treated with PIR3.5 under any condition (Supplementary Fig. S14).

The impact of IPA-3 on the microimpedance signal was cell-type dependent and time dependent. In HeLa cells, pretreatment with IPA-3 (setting 1, left) induced a progressive delay in cell attachment (Fig. 10a). At the highest dose (50 µM), the effect of IPA-3 approached that of dasatinib. In the setting 2 (right), IPA-3 up from 20 µM induced a distinct increase of the signal followed by a decrease, forming a large peak. More complex course occurred in HEK293T cells, which have higher PAK1 content (Supplementary Fig. S8). Cell pretreatment with low-dose IPA-3 did not prevent rapid cell attachment, but reduced the subsequent cell spreading. At 50 µM concentration, the effect of IPA-3 pretreatment was similar as in HeLa cells, close to that of dasatinib (Fig. 10b, left). In the setting 2 (Fig. 10b, right), an immediate signal drop occurred after IPA-3 addition, followed by one or two slower peaks. Although a small drop was usually also detectable in HeLa cells, its amplitude was significantly smaller (mean reduction by 60% in HEK293T versus 18% in HeLa cells after 20 µM IPA-3 addition, $p = 0.008$ from unpaired parametric t-test with Welch's correction, $p = 0.0357$ from Mann-Whitney test). Despite higher efficiency in inhibition of PAK kinase activity, FRAX597 had less marked effect on the microimpedance signal: no delay in cell attachment was observed for pretreated cells (Fig. 10, left, light blue lines) and only a transient increase without any drop occurred after FRAX597 addition to adhered cells (Fig. 10, right).

Figure 11a illustrates the evolution of the ECIS signal in HEK293T cells treated with siRNA to reduce PAK1 or PAK2 expression. The adhesion experiments were performed 24 or 48 h after siRNA transfection. The same cell number was seeded for all samples as checked by fluorescent staining of quadruplet sample aliquots. In agreement with the expected reduction of cell spreading, the amplitude of ECIS signal was lower for cells treated with PAK1 siRNA. Also, the fast drop of the signal after dasatinib addition was smaller in cells transfected with PAK1 siRNA: the mean decrease from 7 experiments was by 32% in the non-targeting control (NT) and by 22% in PAK1 siRNA samples, the reached p-value was 0.05 from paired two-tail t-test. PAK2 silencing had no effect on the amplitude of the signal, but we noted a small delay during the first phase of the cell attachment (Fig. 11a, right). This effect

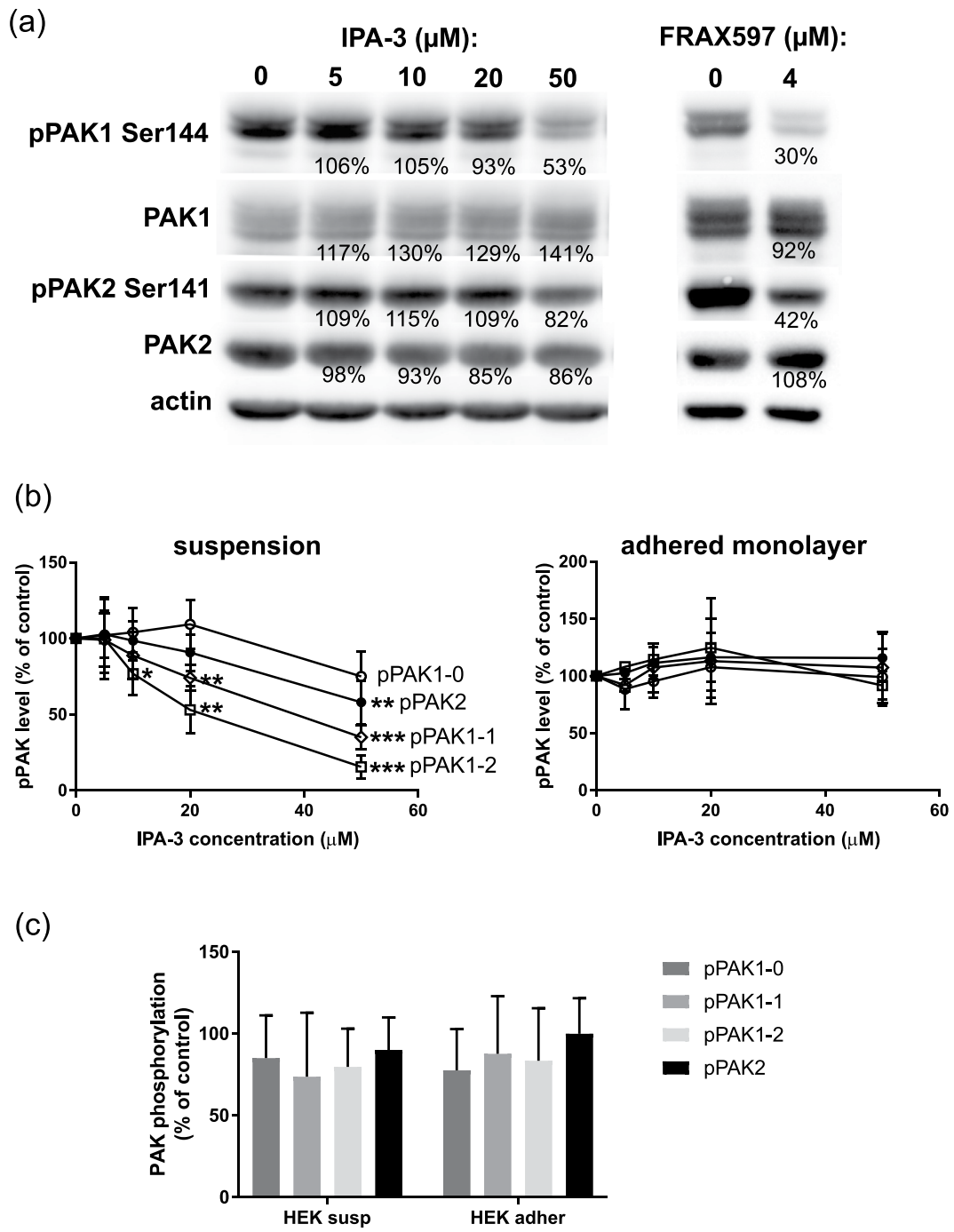


**Figure 9.** Effect of inhibitors on PAK Ser144/Ser141 phosphorylation. HEK293T cells were treated for 30 min with different concentrations of IPA-3, with 4 μM FRAX597, or with 100 nM dasatinib. (**a**) Example of western-blot analysis of Ser144/141 phosphorylation in cells treated in suspension with IPA-3 or FRAX597. The numbers indicate the relative intensity of the signal compared to the untreated control, corrected to loading controls (actin). (**b**) Summary and statistical evaluation of repeated experiments for IPA-3-treated HEK293T cells. The individual phospho-PAK bands are defined in Fig. 1b. Open symbols: circles - pPAK1-0, diamonds - pPAK1-1, squares – pPAK1-2. Closed symbols: pPAK2. Left: HEK293T cells treated in suspension, right: treated as an adhered monolayer. (**c**) Summary of results obtained for dasatinib-treated HEK293T cells, in suspension or in adhered monolayer as indicated. Differences between treated samples and controls were evaluated by paired t-test. *$p < 0.05$, **$p < 0.01$, ***$p < 0.001$.

was less marked in comparison with changes induced by siRNA PAK1, maybe due to lower efficiency in reducing the activity of PAK2. Nevertheless, similar course was observed in 5 of 6 experiments performed 48 h after the cell transfection with siRNA PAK2. The time to reach the local maximum of the signal was significantly larger in cells

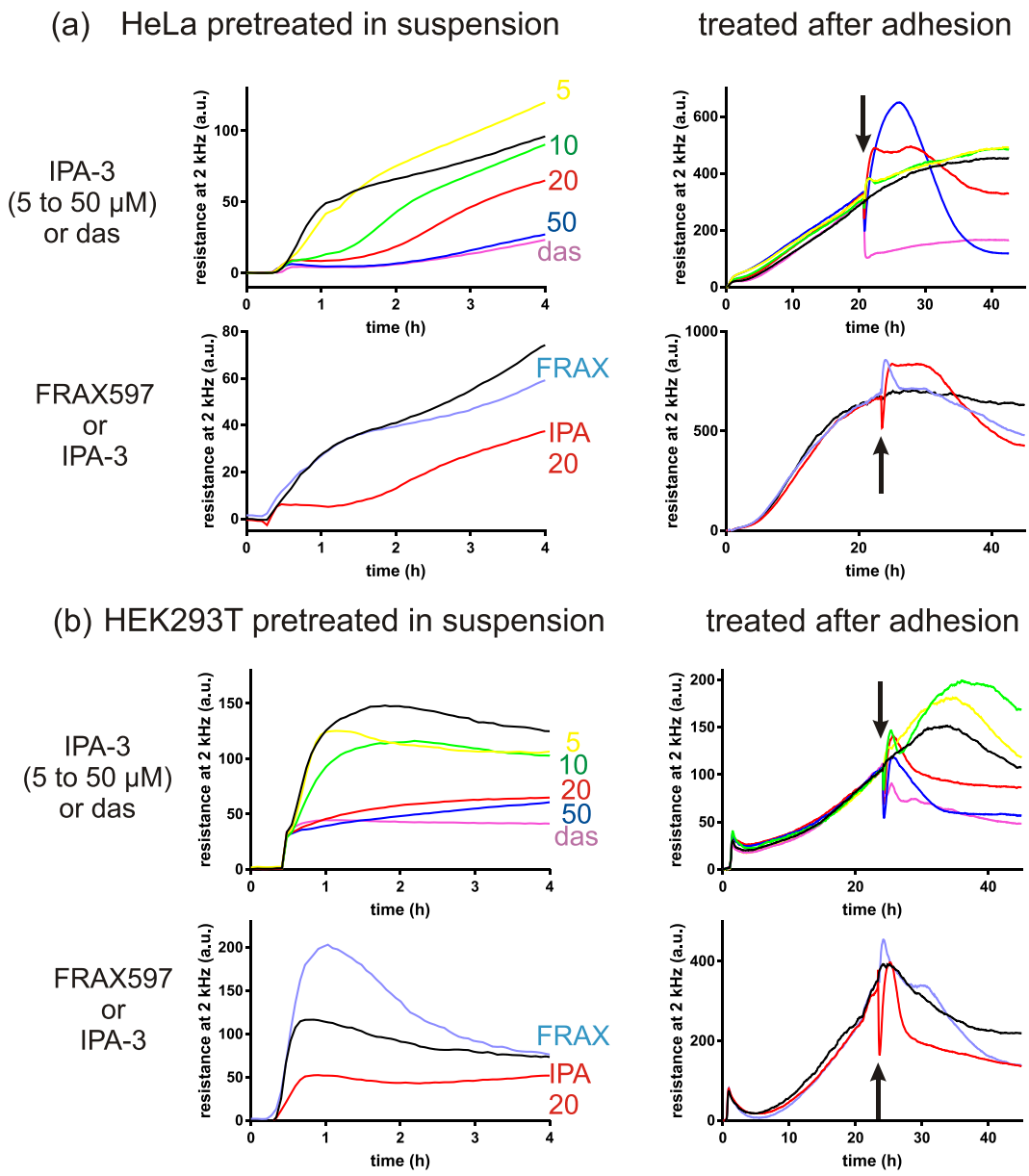


**Figure 10.** Representative records from cell attachment monitoring by ECIS. HeLa cells (**a**) or HEK293T cells (**b**) were preatreated for 30 min with inhibitors before seeding to ECIS wells (left) or treated during measurement (right). The arrows mark the time of inhibitor addition. Color legend: controls: black, IPA-3 at 5 – 10 – 20 – 50 µM: yellow – green – red – blue, dasatinib 100 nM: magenta, FRAX597 4 µM: light blue.

treated with siRNA PAK2 (mean value 0.58 h compared to 0.43 h in cells treated with the non-targeting siRNA, $p = 0.0059$ from paired t-test). On the other hand, no significant change of this parameter was observed in cells treated with siRNA PAK1.

PAK1 splicing is mediated by the splicing factor U2AF65, the activity of this factor being modulated by the lysyl-hydroxylase JMJD6. JMJD6 silencing in melanoma cells resulted in an increased transcript level of PAK1Δ15 compared to the full-length form[41]. We thus tested the effect of JMJD6 silencing by siRNA in HEK293T cells on PAK expression at the protein level and on its phosphorylation, as well as on cell adhesion. The effect of JMJD6 silencing on PAK band pattern is shown in the Supplementary Fig. S15 (representative example from 4 repeated experiments). The overall PAK1 expression level did not significantly change and no additional band attributable to PAK1Δ15 was detected, but the highest PAK1 band was reduced. In addition, a marked loss of Ser144/141 phosphorylation was evident on PAK1 and, to a lesser extent, on PAK2. Accordingly, largely lower amplitude of the ECIS signal was observed in cells treated with JMJD6 siRNA (Fig. 11b). Finally, we compared the adhesion of cells transfected with plasmids for expression of PAK1-full, PAK1Δ15 or PAK2 (all GFP-labeled) (Fig. 11c). The transfection efficiency was checked by flow-cytometry, about 70% of cells produced a high amount of fluorescent proteins at 24 h after transfection. The same cell number was seeded in quadruplicates in ECIS

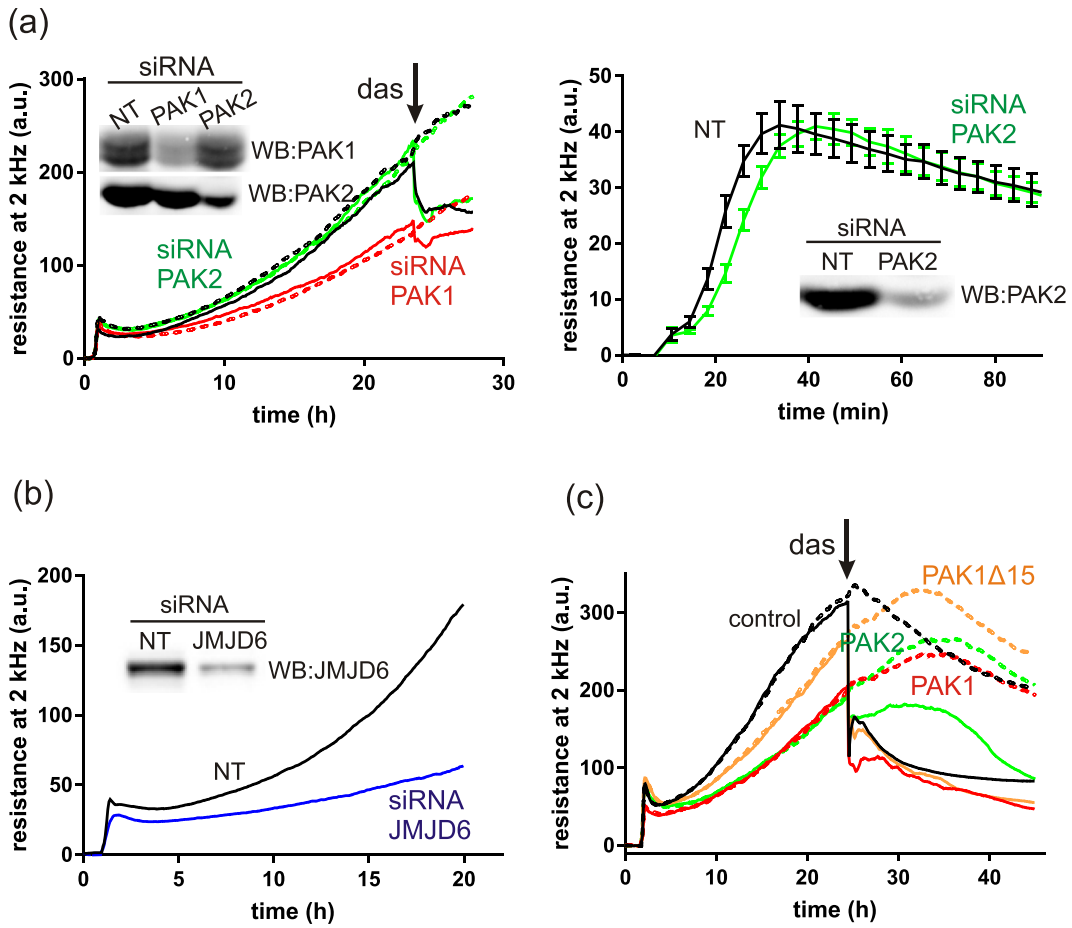


**Figure 11.** Attachment of HEK293T cells transfected with siRNA, or with plasmids for exogenous PAK expression. All samples were seeded in quadruplicates, the lines represent the means. (**a**) Effect of siRNA PAK1 and siRNA PAK2 on ECIS signal. Black: non-targeting siRNA (NT), red: siRNA PAK1, green: siRNA PAK2. In the left image, 100 nM dasatinib was added to the wells, that are represented by solid lines, at the time point indicated by the arrow. (**b**) Effect of siRNA JMJD6 on ECIS signal. Black: NT, blue: siRNA JMJD6. (**c**) Effect of PAK overexpression on ECIS signal. Black: control without plasmid, red: PAK1-full-eGFP, orange: PAK1Δ15-eGFP, green: PAK2-eGFP. The arrow indicates the time point of 100 nM dasatinib addition to the wells represented by solid lines. The Figure shows representative examples of repeated experiments (N = 7 for siRNA PAK1, N = 6 for siRNA PAK2, N = 4 for siRNA JMJD6, and N = 3 for each type of plasmid).

wells, and dasatinib was added to two of the four wells 24 h later. Decreased and/or delayed cell spreading was observed for all PAK-transfected samples compared to the cells treated without any plasmid, the largest effect being associated with PAK1-full.

## Discussion

PAK group I were discovered as effectors of small GTPases of the Rho family, which are the principal regulators of processes associated with cytoskeleton dynamics, such as cell adhesion and migration. In particular, the founding member of the PAK family, PAK1, has been analyzed in detail in this context. To date, PAK1 has well-established roles in the formation of plasma membrane protrusions[46–48], actin stress fiber dissolution and focal adhesion reorganization[49]. PAK1 kinase activity appears necessary for disassembly of focal adhesions and of actin stress fibers, whereas membrane ruffling and lamellipodia formation are kinase independent[50].

Theoretically, multiple protein isoforms can be formed from the PAK1 gene. Both Swissprot and NCBI annotate two splicing isoforms, which give raise to the full-length PAK1 (553 AA) and to the variant lacking the exon 15, which is denoted as PAK1Δ15 (545 AA). In the majority of studies, these variants are not distinguished, despite possible differences in their functions. The ratio between PAK1-full and PAK1Δ15 transcripts was reported to be regulated by the demethylase/hydroxylase JMJD6 in melanoma[41]. In the same study, increased JMJD6 expression was associated with more aggressive disease and with worse survival in melanoma patients. JMJD6 was found to increase the PAK1-full/PAK1Δ15 ratio, to enhance MAPK signaling and to promote proliferation and invasion of melanoma cells.

PAK2 is known to be involved in the apoptosis[26,51,52]. However, only a limited number of studies focused on specific functions of PAK2 in cell adhesion. The roles of PAK1 and PAK2 were analyzed in detail using siRNAs in a lung carcinoma model[8]. Both PAK1 and PAK2 were required for heregulin-induced cell invasiveness, but many

differences were observed in the mechanisms of their functions. PAK1 mediated cofilin dephosphorylation, and had stronger effect on lamellipodia formation. PAK2 was involved in the formation of new focal adhesions after heregulin stimulation and suppressed the activity of RhoA. PAK1 and PAK2 also had opposed effects on the myosin light chain phosphorylation.

In the present work, we aimed to characterize PAK1-full, PAK1Δ15 and PAK2 using several complementary approaches. We prepared plasmids for exogenous expression of all these kinases and compared PAK intracellular localization (Figs. 7, 8, and S7). Furthermore, we used the eGFP- and mCherry-tagged isoforms to analyze their mutual interactions using co-immunoprecipitation (Fig. 5). Functional differences between PAK1 and PAK2 were assessed using siRNA-mediated reduction of protein expression and by comparison of two cell lines, HEK293T and HeLa, the latter having much lower PAK1 expression than the former (Supplementary Fig. S8).

Antibodies against PAK1 detected at least three different bands in western-blots (Figs. 1 and 3), that could correspond to splicing variants, but also to different activation stages. The electrophoretic mobility of recombinant PAK1 was described to change after *in vitro* activation by Cdc42[10,49]. The existence of several PAK1 bands is generally believed to be due to multiple phosphorylation events occurring during the kinase activation. PAK1 has at least seven autophosphorylation sites (Ser21, Ser57, Ser144, Ser149, Ser199, Ser204 and Tyr423), and thirteen phosphorylated residues were found in a mass-spectrometry screen[53]. However, although equivalent phosphorylation sites are for the most present on PAK2, this protein is detected in a single dominant band. To check the association between PAK1 phosphorylation and the band position on western-blots, we used alkaline phosphatase (AP) treatment (Fig. 4). The extent of phosphorylation at Ser144 and at Thr212 was markedly reduced by overnight treatment with 2250 U of AP. Although the majority of PAK bands were actually slightly shifted to a lower apparent MW, they remained distinctly separated. This result suggests that the hyperphosphorylation is not the main cause of the band multiplicity. Instead, other posttranslational modification could occur during PAK1 activation, possibly similar to PAK2 myristoylation upon caspase-mediated cleavage[42]. We have also noted that the affinity of some antibodies to PAK1 is affected by phosphorylation (e.g. ab223849, Fig. 4). With regard to the complex band pattern in cells with exogenous PAK1 expression, it is not clear if the naturally occurring bands are derived from PAK1-full or PAK1Δ15. A mix of both may be present, the band position being further influenced by protein activation and phosphorylation. As the highest PAK1 band was reduced by JMJD6 silencing (Supplementary Fig. S15), it could originate from PAK1-full. On the transcript level, PAK1Δ15 was found to be dominant (Supplementary Fig. S3), and it is thus not surprising that the overall PAK1 signal was not largely modified after JMJD6 siRNA treatment. The unchanged lower bands could correspond to PAK1Δ15 (Figs. 3 and 4).

The intracellular localization of the eGFP-tagged PAK1-full is in agreement with the current knowledge about PAK1 function, especially with the stimulation of membrane protrusions at the leading edge of migrating cells (Fig. 7b). On the other hand, the localization of PAK1Δ15 was similar to that of PAK2: both these kinases were enriched in focal adhesions (FA) (Figs. 7, 8b, and S7). With regard to the sequence comparison shown in Fig. 2, targeting to FA could be related to the C-terminal sequence. Interestingly, PAK1 was found in FA in some of the previous works[20,49]. Although the splicing variant was not explicitly defined, the PAK1 form used in these experiments was reported to have 544 AA, and was thus probably derived from PAK1Δ15. The kinase was released from FA upon Akt-mediated phosphorylation at Ser21[20]. PAK2 presence in FA detected in our experiments (Figs. 7, 8 and S7) corresponds to its reported role during assembly of new adhesion points[8].

The significance of homodimers for PAK1 autoinhibition was recently contested by structural analyses of the protein in solution, which suggested that the autoinhibited full-length PAK1 are monomers, whereas dimers are present only transiently to allow for kinase autophosphorylation and full activation[54]. However, PAK1 and PAK2 dimers were easily detectable in our co-immunoprecipitation experiments (Fig. 5) and no PAK1-full monomers were found by native electrophoresis in cell lysates (Fig. 6).

Figure 5 also shows that PAK1-full, PAK1Δ15 and PAK2 mutually interact in all possible combinations. It is thus likely that they also mutually affect their function. In line with this hypothesis, we noted that in cells co-transfected with PAK2/PAK1Δ15 and PAK1-full, only few cells expressed high levels of both kinases simultaneously. The localization of PAK2/PAK1Δ15 (green) in FA was more apparent in the absence of PAK1-full (red) overexpression (Fig. 7b and Supplementary Fig. S7c). Also, PAK2 presence in FA was clearly detected in HeLa cells, but not in HEK293T cells, which express higher amount of endogenous PAK1. Moreover, negative regulation of PAK1 by PAK2 have been suggested in epithelial cells, where PAK2 knock-down increased PAK1 phosphorylation[55]. Similarly, PAK1 was reported to inhibit PAK3 activity in kinase assays[18].

In the co-immunoprecipitation experiments, we also observed truncation of PAK1Δ15, as well as of PAK2, during interaction with PAK1-full (Fig. 5a,b; Table 2). The fragment size was similar to that produced by caspase-mediated cleavage of PAK2. However, the process was probably caspase-independent, as it was unaffected by the inhibitor Q-VD-OPh (Supplementary Fig. S5), which completely blocks caspase activity at the concentration used[56]. Also, PAK1Δ15 sequence does not contain the consensus caspase cleavage site. We cannot exclude the possibility that the truncation was an artifact due to the fluorescence labeling of the PAK molecules, which could result in a steric hinderance altering the dimer conformation. However, virtually identical PAK2 truncation was observed with the inverse labeling. Also, PAK2 was cleaved upon interaction with PAK1-full (Fig. 5a), but not with PAK1Δ15 (Fig. 5c), despite the identical N-terminal part of these PAK1 isoforms (Fig. 2). In any case, if the heterodimer-induced cleavage occurred *in vivo*, the removal of the N-terminal part of PAK2/PAK1Δ15 could have similar consequence as the apoptotic PAK2 cleavage, i.e. constitutive activation of the kinase due to the absence of AID. On the other hand, PAK1Δ15 lacks the myristoylation sequence which could redirect the kinase to cell membranes, as it is the case for caspase-cleaved PAK2[42].

Cell response to an acute PAK inhibition was studied using the relatively specific inhibitor IPA-3[57], which binds to the closed conformation of the protein and prevents kinase activation. Accordingly, the effect of IPA-3 on Ser144/141 phosphorylation was larger for PAK1 bands at lower MW (Fig. 9b), which should correspond to less activated forms[49]. Nevertheless, specific effects of IPA-3 on cell adhesion (Fig. 10) occurred at lower

concentrations than those required for noticeable PAK dephosphorylation at Ser144/141. Also, FRAX597 did not fully reproduce the effects of IPA-3 treatment (Fig. 10). This is consistent with different modes of action of the two inhibitors: FRAX597 only inhibits the kinase activity, whereas IPA-3 presumably prevents all PAK functions. PAK activation is a multistage process and Ser144/141 phosphorylation stabilizes the final open conformation[15]. However, PAK1 also acts as a scaffold, and this function is supposed to be kinase-independent. Indeed, induction of membrane ruffling by PAK1 overexpression was reported to be largely independent of PAK1 kinase activity[3]. IPA-3 treatment also induced an increase in phosphorylation at Ser20 and this effect was already apparent at the lowest IPA-3 doses used (Supplementary Fig. S12), which did not affect Ser144/141 phosphorylation. As it was expected, the control compound PIR3.5 did not induce changes in PAK phosphorylation. The observed effects are thus mostly attributable to PAK inhibition and not to an increased oxidative stress.

The results of our experiments involving small molecule inhibitors (Fig. 10) and siRNA (Fig. 11) are consistent with the following model: PAK1-full regulates cell spreading, presumably by promoting actin remodelling and formation of membrane protrusions, and this function is largely independent of PAK1 kinase activity. PAK2 is required for FA assembly and its depletion/inhibition slows down the cell attachment to the surface. This is in agreement with results obtained previously in another cell type[8]. The roles of PAK1 and PAK2 in cell adhesion are thus not redundant, although these kinases were reported to have virtually identical substrate specificity[58]. It was suggested previously that PAK2 may functionally compensate for PAK1 in neovascularization and wound healing[59]. On the other hand, mutually opposed functions of PAK1 and PAK2 were described for other processes, e.g. in paxillin targeting to extracellular vesicles[60]. The possibility to document differences in functions between PAK1-full and PAK1Δ15 is limited as there is no mean of specific inhibition of these two forms. The exogenously produced proteins are not fully active, probably due to autoinhibition in dimers, and they affect the function of the endogenous proteins, possibly through heterodimer formation (Supplementary Fig. S6). For this reason, the interpretation of functional experiments involving protein overexpression (Fig. 11c) is not obvious. Decreased or delayed ECIS signal could be related to autoinhibition of both exogenous and endogenous PAK1-full by dimer formation. In addition, PAK1-full overexpression may induce cleavage of the endogenous PAK1Δ15/PAK2, with unclear consequences on their activity. Interestingly, ECIS response to dasatinib in Fig. 11c was different in cells with PAK1-full versus PAK2 overexpression: the signal course in the latter case involved a large peak similar to that induced by low-dose IPA-3 treatment (Fig. 10b, right). In general, such evolution of the ECIS signal may be due to an increase in spreading (larger cell area), but also to a closer cell contact with the surface. For example, inhibition of PAK1 kinase activity could result in stabilization of focal adhesions. Direct imaging was performed for dasatinib, where the signal drop was clearly associated with cell shrinking (Supplementary Fig. S13). However, IPA-3 addition increases sample turbidity and direct imaging on Nanolive microscope was thus not feasible. Indirect indication as to the importance of an increase in the cell area versus closer cell attachment is provided by comparison of the resistance and capacitance components of the ECIS signal. In fact, the capacitance at high frequencies of the sensing electrical field depends mainly on changes in the surface coverage (i.e., cell area), whereas the resistance at lower frequencies is more affected by cell-surface contact tightness. The changes we observed after cell treatment with inhibitors were usually more pronounced in the resistance component of the signal at low frequencies (see an example in Supplementary Fig. S17). The cell response to treatment thus probably involves changes in both spreading and attachment force.

In conclusion, our findings indicate important differences between PAK1-full and PAK1Δ15, the latter being in some aspects closer to PAK2 than to PAK1-full (Figs. 5 and 8, Table 2). This highlights the importance of the C-terminal sequence for PAK behaviour (Fig. 2). Furthermore, all the studied PAK group I isoforms probably mutually affect their functions, which are rather complementary than redundant. PAK1 also undergoes still unknown posttranslantional modification other than phosphorylation, as it is suggested by at least two distinct bands in western-blots (Figs. 3, 4, 6, and 9).

## Material and Methods

**Cell culture.** HeLa and HEK293T cells were obtained as a gift and authenticated using analysis of short tandem repeats, the results were compared with ATCC database. The cells were cultured in the recommended medium (RPMI-1640 for HeLa, DMEM for HEK293T) with 10% fetal calf serum, 100 U/ml penicillin and 100 µg/ml streptomycin at 37 °C in 5% $CO_2$ humidified atmosphere. Cells from resuscitated frozen aliquots were not passaged for more than 3 months.

**Inhibitors and antibodies.** IPA-3 (#3622) and PIR3.5 (#4212) were purchased from Tocris Bioscience and dissolved in sterile dimethylsulfoxide (DMSO) to make 50 mM stock solutions. Working solutions were prepared by 10 fold dilution of the stock solution in 50 mM Tris, pH 8.0, immediately before use. The cell density was adjusted to $3 \times 10^5$ cells/ml for all experiments involving IPA-3 and PIR3.5 treatment. FRAX597 (#6029) was purchased from Tocris Biosciences and dissolved in sterile DMSO to make 10 mM stock solution. Working solution was prepared by dilution in cell culture medium.

Dasatinib was obtained from Selleckchem (#S1021), 200 µM stock solution was made in sterile DMSO. The antibodies against PAK1/2 are specified in Table 1. Other antibodies were purchased from the following providers: JMJD6 (sc 28348) and GFP (sc-9996) from Santa Cruz, β-actin (A5441) from Sigma-Aldrich, PAK3 from Cell Signaling (#2609). Anti-RFP was from Santa Cruz (sc-390909) or from Chromotek (6G6).

**Plasmid preparation and cell transfection.** DNA fragments coding for PAK1-full, PAK1Δ15, and PAK2 were amplified from cDNA library (Jurkat cells, Origene) by PCR, using merged primers containing appropriate restriction sites (PAK1, both isoforms, Fw: AAAAAAAAGCTTCATGTCAAATAACGGCCTAGACA; Pak1-full Rv: AAAAAAGGATCCCGCTGCAGCAATCAGTGGA; PAK1Δ15 Rv: AAAAAAGGATCCCGTGATTGTTCTTT GTTGCCTCC; PAK2 Fw: AAAAAACTCGAGCATGTCTGATAACGGAGAACTG, Rv: AAAAAAGGATCCCAC

GGTTACTCTTCATTGCTTCT). To obtain expression of full-length proteins with no tag, the stop codon TAA was introduced into the reverse primers for PCR amplification of both PAK1 isoforms. The fragments were inserted into vectors peGFP-N2 or pmCherry-N2 (originally Clontech) designed for expression of proteins tagged with eGFP and mCherry at the C-terminus by standard methods of molecular cloning. Resulting plasmids were amplified in E. coli and purified with the PureYield Plasmid Miniprep System (Promega). The plasmids were then transfected into HEK293T cells using jetPRIME transfection reagent (Polyplus Transfection) following the manufacturer's instructions. ON-TARGETplus siRNA (Dharmacon) targeting PAK1 (#L-003521), PAK2 (#L-003597), or JMJD6 (#L-010363), in parallel with a non-targeting control (#D-001810), were transfected using the same reagent (jetPRIME). The concentration range for siRNA was 100–150 nM (final concentration during transfection). The cells were then cultivated for 24 to 48 h without changing medium and harvested for further analyses.

**Western-blotting.** The cells, when in suspension, were pelleted by centrifugation, washed once with ice-cold HBS (HEPES – buffered saline; 20 mM HEPES, 150 mM NaCl, pH 7.1) and lysed for 10 min/4 °C in Pierce IP Lysis Buffer (#87787) with freshly added protease and phosphatase inhibitors. When cultured on a plate in adherent layer, the cells were washed directly in the plate and scrapped into the lysis buffer. The suspension was then transferred to a centrifugation tube and incubated for 10 min/4 °C. Cellular debris was removed by centrifugation (15.000 g/4 °C/15 min), the lysate was mixed 1:1 (v/v) with 2x Laemmli sample buffer and incubated for 5 min at 95 °C.

An equivalent of 20 µg of total protein was resolved on 7.5% polyacrylamide gel (18 × 18 cm) and transferred to a nitrocellulose membrane. The membrane was blocked for 1 h in 3% bovine serum albumin and incubated for 1 h with the primary antibody in PBS with 0.1% Tween-20 (PBST), at the room temperature. Thereafter, it was washed in PBST six times and incubated with the corresponding HRP-conjugated secondary antibody for 1 h. The chemiluminiscence signal from Clarity Western ECL Substrate (BioRad, #170-5060) was detected and analyzed using G:BOX iChemi XT-4 (Syngene).

**Alkaline phosphatase (AP) treatment of cell lysates.** The cells were lysed as described in the western-blotting section. After centrifugation, lysates were diluted five fold in AP buffer (5 mM TRIS HCl, 30 mM NaCl, 1.5 mM MgCl2, 0.2% NP-40, 0.2 mM EDTA, 1% glycerol; pH 8.0) and treated with ~2250 U AP (for the protein yield from $1 \times 10^6$ cells). The samples were incubated at 37 °C for 20 to 24 h. The reaction was stopped by addition of 2x Laemmli sample buffer followed by incubation at 95 °C for 5 min.

**Electrical cell-substrate impedance sensing (ECIS).** Impedance measurements were performed using the ECIS Zθ device (Applied Biophysics). The wells of a 8W10E + plate were filled with 200 µl culture medium and the baseline was monitored for several hours before cell addition. In the setting 1, the medium was removed and 400 µl of cell suspension was added. In this setting, the cells were pretreated for 30 min with inhibitors. In parallel, aliquots of cell suspensions were used to check for equal cell numbers by fluorescent staining (CyQuant Cell Proliferation Assay Kit; Molecular Probes, #C7026). In the setting 2, the cell suspension (200 µl) was added to the wells, the cell attachment was monitored overnight, and the inhibitors were added after 20 to 24 h. One of the wells in each plate were left empty (medium only) and the signal was used as a baseline for the other wells. The instrument automatically decomposes the impedance signal into resistance and capacitance. The ECIS records were exported to Excel and processed using the GraphPad Prism software: the background was set to zero at a time point shortly before cell seeding, and the baseline (empty well) was subtracted. The signals shown in the graphs with inhibitors represent the averages from two identically treated plates, which were run in parallel.

**Confocal microscopy.** Localization of PAK was analyzed by live cell imaging in cells transfected with plasmids for expression of proteins with fluorescent tags and by immunofluorescence in cells fixed with 2% paraformaldehyde and permeabilized with 0.3% Triton X-100.

Interference reflection microscopy (IRM) was used to visualize cell-substrate contact points. The measurement was performed by means of FV-1000 confocal microscope (Olympus), using 405 nm laser beam and focusing to the glass surface.

**Immunoprecipitation.** Immunoprecipitation using GFP- or RFP-Trap (Chromotek) was performed according to manufacturer´s instruction as described previously[61]. Briefly, cells were harvested and washed with PBS, lysed in Lysis buffer (10 mM Tris/Cl pH7.5, 150 mM NaCl, 0.5 mM EDTA, 0.5% NP-40, protease and phosphatase inhibitors) for 30 min/4 °C and centrifuged at 20.000 g/4 °C for 10 min. A small fraction of lysate was put aside for native and SDS-PAGE and the majority of lysate was mixed with GFP/RFP-nanobody-coated beads and rotated for 1 h/4 °C. Then the beads were extensively washed with diluting buffer (10 mM Tris/Cl pH 7.5, 150 mM NaCl, 0.5 mM EDTA), resuspended in Laemmli sample buffer (50 mM Tris pH 6.8, 2% SDS, 100 mM DTT, 10% glycerol), boiled at 95 °C for 10 min and centrifuged 20.000 g/4 °C for 10 min. Supernatant was stored at −20 °C until used for SDS-PAGE.

**Native and semi-native PAGE.** Lysate aliquots obtained during the immunoprecipitation procedure were mixed with 2x native buffer (50 mM Tris pH 6.8, 10 mM DTT, 10% glycerol) and subjected without boiling to 4–15% gradient gel (BioRad) without SDS for native electrophoresis, or to 7.5% polyacrylamide gel with 0.1% SDS for semi-native electrophoresis. After blotting to a PVDF membrane (BioRad), the blot was incubated with GFP primary antibody at a dilution 1:250 or at 1:500 for native or semi-native samples. Anti-mouse HRP-conjugated secondary antibody from Thermo Scientific was used at concentrations 1:20.000 and 1:50.000, respectively. ECL Plus Western Blotting Detection System (GE Healthcare) was used for chemiluminiscence visualization and evaluation by G-box iChemi XT4 digital imaging device (Syngene Europe).

Received: 15 April 2019; Accepted: 30 September 2019;
Published online: 20 November 2019

## References


1. Manser, E., Leung, T., Salihuddin, H., Zhao, Z. S. & Lim, L. A brain serine/threonine protein kinase activated by Cdc42 and Rac1. *Nature* **367**, 40–46 (1994).
2. Knaus, U. G., Morris, S., Dong, H. J., Chernoff, J. & Bokoch, G. M. Regulation of human leukocyte p21-activated kinases through G protein–coupled receptors. *Science* **269**, 221–223 (1995).
3. Bokoch, G. M. Biology of the p21-activated kinases. *Annu. Rev. Biochem.* **72**, 743–781 (2003).
4. Molli, P. R., Li, D. Q., Murray, B. W., Rayala, S. K. & Kumar, R. PAK signaling in oncogenesis. *Oncogene* **28**, 2545–2555 (2009).
5. Radu, M., Semenova, G., Kosoff, R. & Chernoff, J. PAK signalling during the development and progression of cancer. *Nat. Rev. Cancer.* **14**, 13–25 (2014).
6. Singh, R. R., Song, C., Yang, Z. & Kumar, R. Nuclear localization and chromatin targets of p21-activated kinase 1. *J. Biol. Chem.* **280**, 18130–18137 (2005).
7. Kumar, R. & Li, D. Q. PAKs in Human Cancer Progression: From Inception to Cancer Therapeutic to Future Oncobiology. *Adv. Cancer Res.* **130**, 137–209 (2016).
8. Coniglio, S. J., Zavarella, S. & Symons, M. H. Pak1 and Pak2 mediate tumor cell invasion through distinct signaling mechanisms. *Mol. Cell. Biol.* **28**, 4162–4172 (2008).
9. Arias-Romero, L. E. & Chernoff, J. A tale of two Paks. *Biol. Cell.* **100**, 97–108 (2008).
10. Manser, E. *et al*. PAK kinases are directly coupled to the PIX family of nucleotide exchange factors. *Mol. Cell* **1**, 183–192 (1998).
11. Obermeier, A. *et al*. PAK promotes morphological changes by acting upstream of Rac. *EMBO J.* **17**, 4328–4339 (1998).
12. Lei, M. *et al*. Structure of PAK1 in an autoinhibited conformation reveals a multistage activation switch. *Cell* **102**, 387–397 (2000).
13. Zenke, F. T., King, C. C., Bohl, B. P. & Bokoch, G. M. Identification of a central phosphorylation site in p21-activated kinase regulating autoinhibition and kinase activity. *J. Biol. Chem.* **274**, 32565–32573 (1999).
14. Parrini, M. C., Lei, M., Harrison, S. C. & Mayer, B. J. Pak1 kinase homodimers are autoinhibited in trans and dissociated upon activation by Cdc42 and Rac1. *Mol. Cell* **9**, 73–83 (2002).
15. Parrini, M. C. Untangling the complexity of PAK1 dynamics: The future challenge. *Cell. Logist* **2**, 78–83 (2012).
16. Shin, Y. J., Kim, Y. B. & Kim, J. H. Protein kinase CK2 phosphorylates and activates p21-activated kinase 1. *Mol. Biol. Cell* **24**, 2990–2999 (2013).
17. Harms, F. L. *et al*. Activating Mutations in PAK1, Encoding p21-Activated Kinase 1, Cause a Neurodevelopmental Disorder. *Am. J. Hum. Genet.* **103**, 579–591 (2018).
18. Combeau, G. *et al*. The p21-activated kinase PAK3 forms heterodimers with PAK1 in brain implementing trans-regulation of PAK3 activity. *J. Biol. Chem.* **287**, 30084–30096 (2012).
19. Puto, L. A., Pestonjamasp, K., King, C. C. & Bokoch, G. M. p21-activated kinase 1 (PAK1) interacts with the Grb2 adapter protein to couple to growth factor signaling. *J. Biol. Chem.* **278**, 9388–9393 (2003).
20. Zhou, G. L. *et al*. Akt phosphorylation of serine 21 on Pak1 modulates Nck binding and cell migration. *Mol. Cell. Biol.* **23**, 8058–8069 (2003).
21. Tao, J., Oladimeji, P., Rider, L. & Diakonova, M. PAK1-Nck regulates cyclin D1 promoter activity in response to prolactin. *Mol. Endocrinol.* **25**, 1565–1578 (2011).
22. Hammer, A., Oladimeji, P., De Las Casas, L. E. & Diakonova, M. Phosphorylation of tyrosine 285 of PAK1 facilitates betaPIX/GIT1 binding and adhesion turnover. *FASEB J.* **29**, 943–959 (2015).
23. Banerjee, M., Worth, D., Prowse, D. M. & Nikolic, M. Pak1 phosphorylation on t212 affects microtubules in cells undergoing mitosis. *Curr. Biol.* **12**, 1233–1239 (2002).
24. King, C. C. *et al*. p21-activated kinase (PAK1) is phosphorylated and activated by 3-phosphoinositide-dependent kinase-1 (PDK1). *J. Biol. Chem.* **275**, 41201–41209 (2000).
25. Rudel, T. & Bokoch, G. M. Membrane and morphological changes in apoptotic cells regulated by caspase-mediated activation of PAK2. *Science* **276**, 1571–1574 (1997).
26. Hsu, Y. H., Johnson, D. A. & Traugh, J. A. Analysis of conformational changes during activation of protein kinase Pak2 by amide hydrogen/deuterium exchange. *J. Biol. Chem.* **283**, 36397–36405 (2008).
27. Wilkes, M. C., Murphy, S. J., Garamszegi, N. & Leof, E. B. Cell-type-specific activation of PAK2 by transforming growth factor beta independent of Smad2 and Smad3. *Mol. Cell. Biol.* **23**, 8878–8889 (2003).
28. Chan, W. H., Yu, J. S. & Yang, S. D. PAK2 is cleaved and activated during hyperosmotic shock-induced apoptosis via a caspase-dependent mechanism: evidence for the involvement of oxidative stress. *J. Cell. Physiol.* **178**, 397–408 (1999).
29. Tang, T. K. *et al*. Proteolytic cleavage and activation of PAK2 during UV irradiation-induced apoptosis in A431 cells. *J. Cell. Biochem.* **70**, 442–454 (1998).
30. Roig, J. & Traugh, J. A. Cytostatic p21 G protein-activated protein kinase gamma-PAK. *Vitam. Horm.* **62**, 167–198 (2001).
31. Marlin, J. W., Eaton, A., Montano, G. T., Chang, Y. W. & Jakobi, R. Elevated p21-activated kinase 2 activity results in anchorage-independent growth and resistance to anticancer drug-induced cell death. *Neoplasia* **11**, 286–297 (2009).
32. Marlin, J. W. *et al*. Functional PAK-2 knockout and replacement with a caspase cleavage-deficient mutant in mice reveals differential requirements of full-length PAK-2 and caspase-activated PAK-2p34. *Mamm. Genome* **22**, 306–317 (2011).
33. Li, X. *et al*. Phosphorylation of caspase-7 by p21-activated protein kinase (PAK) 2 inhibits chemotherapeutic drug-induced apoptosis of breast cancer cell lines. *J. Biol. Chem.* **286**, 22291–22299 (2011).
34. Ye, D. Z. & Field, J. PAK signaling in cancer. *Cell. Logist* **2**, 105–116 (2012).
35. Huynh, N. *et al*. Depletion of p21-activated kinase 1 up-regulates the immune system of APC(14/+) mice and inhibits intestinal tumorigenesis. *BMC Cancer* **17**, 431-017-3432-0 (2017).
36. Pandolfi, A. *et al*. PAK1 is a therapeutic target in acute myeloid leukemia and myelodysplastic syndrome. *Blood* **126**, 1118–1127 (2015).
37. Semenova, G. & Chernoff, J. Targeting PAK1. *Biochem. Soc. Trans.* **45**, 79–88 (2017).
38. Maruta, H. & Ahn, M. R. From bench (laboratory) to bed (hospital/home): How to explore effective natural and synthetic PAK1-blockers/longevity-promoters for cancer therapy. *Eur. J. Med. Chem.* **142**, 229–243 (2017).
39. Zandvakili, I., Lin, Y., Morris, J. C. & Zheng, Y. Rho GTPases: Anti- or pro-neoplastic targets? *Oncogene* **36**, 3213–3222 (2017).
40. Kumar, R., Sanawar, R., Li, X. & Li, F. Structure, biochemistry, and biology of PAK kinases. *Gene* **605**, 20–31 (2017).
41. Liu, X. *et al*. JMJD6 promotes melanoma carcinogenesis through regulation of the alternative splicing of PAK1, a key MAPK signaling component. *Mol. Cancer.* **16**, 175-017-0744-2 (2017).
42. Vilas, G. L. *et al*. Posttranslational myristoylation of caspase-activated p21-activated protein kinase 2 (PAK2) potentiates late apoptotic events. *Proc. Natl. Acad. Sci. USA* **103**, 6542–6547 (2006).
43. Kuzelova, K., Grebenova, D., Holoubek, A., Roselova, P. & Obr, A. Group I PAK inhibitor IPA-3 induces cell death and affects cell adhesivity to fibronectin in human hematopoietic cells. *PLoS One* **9**, e92560 (2014).
44. Licciulli, S. *et al*. FRAX597, a small molecule inhibitor of the p21-activated kinases, inhibits tumorigenesis of neurofibromatosis type 2 (NF2)-associated Schwannomas. *J. Biol. Chem.* **288**, 29105–29114 (2013).

45. Roselova, P., Obr, A., Holoubek, A., Grebenova, D. & Kuzelova, K. Adhesion structures in leukemia cells and their regulation by Src family kinases. *Cell. Adh Migr.* **12**, 286–298 (2018).
46. Sells, M. A. *et al*. Human p21-activated kinase (Pak1) regulates actin organization in mammalian cells. *Curr. Biol.* **7**, 202–210 (1997).
47. Parrini, M. C., Camonis, J., Matsuda, M. & de Gunzburg, J. Dissecting activation of the PAK1 kinase at protrusions in living cells. *J. Biol. Chem.* **284**, 24133–24143 (2009).
48. Nicholas, N. S. *et al*. PAK4 suppresses PDZ-RhoGEF activity to drive invadopodia maturation in melanoma cells. *Oncotarget* **7**, 70881–70897 (2016).
49. Manser, E. *et al*. Expression of constitutively active alpha-PAK reveals effects of the kinase on actin and focal complexes. *Mol. Cell. Biol.* **17**, 1129–1143 (1997).
50. Frost, J. A., Khokhlatchev, A., Stippec, S., White, M. A. & Cobb, M. H. Differential effects of PAK1-activating mutations reveal activity-dependent and -independent effects on cytoskeletal regulation. *J. Biol. Chem.* **273**, 28191–28198 (1998).
51. Walter, B. N. *et al*. Cleavage and activation of p21-activated protein kinase gamma-PAK by CPP32 (caspase 3). Effects of autophosphorylation on activity. *J. Biol. Chem.* **273**, 28733–28739 (1998).
52. Lee, N. *et al*. Activation of hPAK65 by caspase cleavage induces some of the morphological and biochemical changes of apoptosis. *Proc. Natl. Acad. Sci. USA* **94**, 13642–13647 (1997).
53. Mayhew, M. W. *et al*. Identification of phosphorylation sites in betaPIX and PAK1. *J. Cell. Sci.* **120**, 3911–3918 (2007).
54. Sorrell, F. J., Kilian, L. M. & Elkins, J. M. Solution structures and biophysical analysis of full-length group A PAKs reveal they are monomeric and auto-inhibited in cis. *Biochem. J* (2019).
55. Bright, M. D., Garner, A. P. & Ridley, A. J. PAK1 and PAK2 have different roles in HGF-induced morphological responses. *Cell. Signal.* **21**, 1738–1747 (2009).
56. Kuzelova, K., Grebenova, D. & Brodska, B. Dose-dependent effects of the caspase inhibitor Q-VD-OPh on different apoptosis-related processes. *J. Cell. Biochem.* **112**, 3334–3342 (2011).
57. Deacon, S. W. *et al*. An isoform-selective, small-molecule inhibitor targets the autoregulatory mechanism of p21-activated kinase. *Chem. Biol.* **15**, 322–331 (2008).
58. Rennefahrt, U. E. *et al*. Specificity profiling of Pak kinases allows identification of novel phosphorylation sites. *J. Biol. Chem.* **282**, 15667–15678 (2007).
59. Elsherif, L. *et al*. Potential compensation among group I PAK members in hindlimb ischemia and wound healing. *PLoS One* **9**, e112239 (2014).
60. Lee, J. H. *et al*. HIV Nef, paxillin, and Pak1/2 regulate activation and secretion of TACE/ADAM10 proteases. *Mol. Cell* **49**, 668–679 (2013).
61. Brodska, B., Kracmarova, M., Holoubek, A. & Kuzelova, K. Localization of AML-related nucleophosmin mutant depends on its subtype and is highly affected by its interaction with wild-type NPM. *PLoS One* **12**, e0175175 (2017).


## Acknowledgements

The authors wish to thank M. Voráčová and P. Otevřelová for expert technical assistance, and to H. Čechová for cell line authentication. The work was supported by the Grant Agency of the Czech Republic (grant No 16-16169S) and by the Ministry of Health of the Czech Republic (project for conceptual development of the research organization No 00023736). A version of the manuscript is freely available online as a pre-print at the following link: https://www.biorxiv.org/content/10.1101/580928v1.

## Author contributions

D.G. performed the majority of western-blotting experiments, A.H. designed and constructed the plasmids, P.R. performed microscopy experiments, A.O. performed microimpedance measurements, B.B. performed immunoprecipitation experiments and native electrophoresis, K.K. designed the study, analyzed the results and wrote the manuscript. All authors reviewed the manuscript.

## Competing interests

The authors declare no competing interests.

## Additional information

**Supplementary information** is available for this paper at https://doi.org/10.1038/s41598-019-53665-6.

**Correspondence** and requests for materials should be addressed to K.K.

**Reprints and permissions information** is available at www.nature.com/reprints.

**Publisher's note** Springer Nature remains neutral with regard to jurisdictional claims in published maps and institutional affiliations.